International Journal of Quantum Foundations **12** (2026) 150-178

Original Paper

Helical Phase Geometry of Electrons: A Geometric Interpretation of Quantum and Relativistic Structures

Natarajan T S

Indian Institute of Technology, Madras/Tirupati, India
E-mail: tsniit@iittp.ac.in

Received: 9 February 2026 / Accepted: 20 February 2026 / Published: 22 February 2026

Abstract: A geometric interpretation of electron dynamics is presented based on phase-coherent helical motion constrained by relativistic kinematics. Building on de Broglie's concept of internal periodicity and the Hamilton–Jacobi formulation of mechanics, the electron is modeled as an intrinsic light-speed helical trajectory whose axial pitch corresponds to the de Broglie wavelength and whose transverse scale is set by the reduced Compton length. Within this framework, spin-1/2 symmetry, magnetic moment, rest energy, and bound-state quantization emerge as interconnected consequences of phase closure and geometric constraints, rather than as independent postulates. The formal operator structure of quantum mechanics is recovered as a statistical description of ensembles of phase-coherent helical trajectories, with momentum and energy operators arising as generators of spatial and temporal phase evolution. The framework provides a geometric visualization of interference, tunneling, and quantum transitions, while remaining fully consistent with the standard probabilistic predictions of quantum mechanics and the Lorentz invariance of special relativity. The helical phase interpretation is intended as a conceptual and pedagogical complement to orthodox formalisms, offering physical intuition for otherwise abstract quantum structures without modifying their mathematical foundations. Thus, this work does not propose a modification of quantum theory, but offers a geometric interpretation of its formal structures aimed at clarifying their physical content.

Keywords: Helical electron model; geometric interpretation of quantum mechanics; de Broglie wavelength; zitterbewegung; spin-$\frac{1}{2}$ symmetry;

Lorentz invariance; phase quantization; standing helical waves; wave–particle duality

1. Introduction

Quantum Mechanics (QM) has transformed modern physics. Yet, key questions about the intrinsic structure of electrons, their charge, spin, and wave-particle duality, remain unresolved. Additionally, a simple classical visualization and the interpretation of the theory becomes difficult for learners. This work approaches these issues by adopting an intuitive model in which electrons move helically, combining an internal circular motion (responsible for spin) with an overall linear translation. Inspired by de Broglie, Dirac, and Schrödinger's zitterbewegung [1–3], this work proposes that the electron follows a classical helical geodesic at light speed. This internal luminal motion is responsible for rest energy, spin, and quantization. The helical picture restores geometric visualization to quantum mechanics, while preserving its predictive structure. In addition, the ideas of time dilation and mass increase with velocity, as presented in Special Relativity (SR), emerge as a simple consequence of the postulated internal motion [4]. The present work builds on the earlier analysis by the author on the complex wavefunction and its potential geometric interpretation [5,6].

1.1. Fundamental Role of c

In special relativity, the speed of light c represents the ultimate limit that no material particle can exceed. Einstein's assertion of light-speed invariance across all inertial frames led to the formulation of the invariant space-time interval. Experimental evidence of time dilation and relativistic mass increase shows that the same invariant structure also governs massive particles such as electrons and muons. Dirac's relativistic quantum theory suggests that electrons have instantaneous velocity components of $\pm c$ even while their mean speed is $v < c$, and Schrödinger's zitterbewegung (ZB)—the rapid trembling motion—supports the idea that electrons are structured dynamic entities rather than featureless points.

Although Einstein's $E = mc^2$ naturally follows from Lorentz transformations, QM typically postulates the relativistic energy–momentum relation rather than deriving it from a microscopic geometric model.; the non-relativistic Schrödinger theory uses classical kinetic energy $p^2/2m$ and relativistic QM takes $E^2 = p^2c^2 + m^2c^4$ as a starting point without explaining mass-energy equivalence [7,8]. This gap highlights the need for concepts that bridge quantum and relativistic descriptions.

1.2. Helical Structures Across Scales

Helical trajectories appear across many scales, suggesting a fundamental organizing principle in nature. For example, the Sun's path through the Galaxy is more accurately described as a helix than as a simple closed orbit, since the solar system itself drifts through the galactic environment. When Earth's orbital motion is combined with this galactic drift, the result is a helical path for our planet [9–12]. At the microscopic level, many organisms, including Escherichia coli and sperm use helical propulsion and hydrodynamic analyses indicate that this motion can be energetically optimal in viscous media [13–17]. The recurrence of helical motion, from large astronomical objects down to biological scales, suggests that quantum particles such as electrons may also follow helical dynamics as a fundamental organizational motif.

2. Core Principles of the Model

The model is built on five core principles. These principles should be understood as geometric constraints used for interpretation, not as additional physical postulates beyond standard quantum mechanics.

(1) **Intrinsic Luminal Motion:** An electron possesses an internal circulatory motion with instantaneous tangential speed c when at "rest."

(2) **Invariant Spin:** The associated angular momentum (spin) is invariant across all inertial frames.

(3) **Quantized Action:** The action integrals for internal and external motion are quantized: $\oint p \cdot ds = h/2$ and h, respectively.

(4) **Constant Resultant Velocity:** The vector sum of internal and external velocities is always c.

(5) **Intrinsic Clock:** The internal motion defines the particle's proper time.

3. Mathematical Representation & Key Results

3.1. The Electron at Rest & in Motion

For an electron at rest ($v = 0$), the intrinsic motion is circular, say, in the xy-plane. The quantization of action for one revolution is:

$$S_{\text{int}} = \oint \mathbf{p} \cdot \mathrm{d}s = (m_0 c)(2\pi a_0) = \frac{h}{2}. \tag{3.1}$$

where a_0 and m_0 are the radius and rest mass. The transverse radius of the helical motion is

$$a_0 = \frac{\hbar}{2m_0c}. \tag{3.2}$$

The value of $a_0 = 1.93 \times 10^{-13}$ m. The angular momentum (spin) is:

$$L = |\mathbf{r} \times \mathbf{p}| = a_0(m_0c) = \frac{\hbar}{2}. \tag{3.3}$$

The period T_0 and ZB frequency ω_0 are:

$$T_0 = \frac{2\pi a_0}{c} = \frac{\pi\hbar}{m_0c^2}, \quad \omega_0 = \frac{2\pi}{T_0} = \frac{2m_0c^2}{\hbar}. \tag{3.4}$$

The rest energy, m_0c^2, is equal to the kinetic energy of this internal motion.

3.2. Mathematical Representation of Helix

A helix is generated by superposing sine and cosine waves in perpendicular directions (See Figure 1). Using the imaginary unit $i = \sqrt{-1}$ as a 90° rotation operator, a particle at rest exhibits internal circular motion in the xy plane:

$$x(\tau) = a_0\cos(\omega_0\tau), \quad y(\tau) = a_0\sin(\omega_0\tau), \quad z(\tau) = 0. \tag{3.5}$$

where τ is proper time. The position vector can be written in complex form:

$$\mathbf{r}_{xy}(t) = a_0e^{i\omega_0t}\boldsymbol{\epsilon}_x. \tag{3.6}$$

In a frame S' moving with velocity v along the z-axis, the particle traces a helix:

$$\mathbf{r}(z,t) = a_0e^{-i(kz-\omega t)}\boldsymbol{\epsilon}_x, \quad z = vt. \tag{3.7}$$

Thus the phase $-i(kz - \omega t)$ encodes both spatial and temporal evolution, directly linking the helix geometry to the complex wavefunction:

$$\Psi \sim e^{i(kz-\omega t)}. \tag{3.8}$$

The symbol ψ here denotes the standard quantum wavefunction, reinterpreted geometrically. The spatial part e^{ikz} describes the pitch of the helix (de Broglie wavelength $\lambda = 2\pi/k$), while the temporal part $e^{-i\omega t}$ describes the rotation in the xy-plane (zitterbewegung) [18–20].

4. Quantization from Helical Geometry

Figure 1. Helical trajectory of the electron. A 3D rendering showing the intrinsic helical path with radius $a_0 = \hbar/(2m_0c)$ and pitch equal to the de Broglie wavelength $\lambda = \hbar/p$. Projections on the xz and yz planes appear as sine and cosine waves.

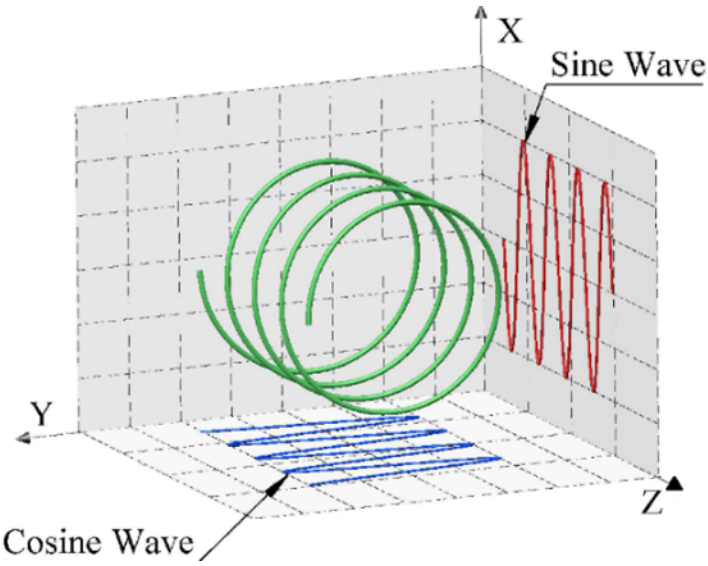

4.1. Particle in a 1D Infinite Potential Well

In the non-relativistic limit, the electron's helical path can be visualized as a geodesic on a cylindrical surface in three-dimensional space. For the full relativistic treatment, the helical trajectory is constrained to be a null geodesic ($ds^2 = 0$) in spacetime, with the cylindrical geometry now representing a world-tube whose cross-section is determined by the Compton wavelength.

This allows the use of the well-known Euler-Lagrange formalism from the calculus of variations to determine the extremal path between two points A and B, separated by an axial distance L along the cylinder [21]. The family of extremal paths includes not just one helix but an infinite series of helices that wind around the cylinder once, twice, thrice, and so on, before reaching the same endpoint. See Figure 2. For a fixed traversal time, the higher-order helices complete multiple revolutions, implying larger tangential velocities and therefore higher momenta. Correspondingly, their de Broglie wavelengths (helical pitches) decrease, as required by the relation $p = \hbar/\lambda$.

Quantized stationary states in the helical model cannot correspond to a single helix propagating indefinitely in one direction. A single helical wave represents a traveling phase field carrying momentum, but such a configuration cannot satisfy the self-consistency conditions required for quantization. Energy eigenstates arise only when two counter-propagating helices superpose coherently to form a standing pattern. In this configuration, the axial phase advances of the two counter-propagating helices cancel each

other, producing stationary nodes and antinodes along the axis, while the internal rotational phase remains coherent. Each quantized state corresponds to an integer number of helical wavelengths fitting within the spatial boundary, leading to discrete energy levels analogous to those of the Schrödinger equation. Figure 3 below highlights the formation of several allowed "standing waves (helices)" corresponding to discrete energies of QM [22].

Thus, for a particle confined between $z = 0$ and $z = L$, the motion is equivalent to two counter-propagating helical waves forming a stationary pattern. At the boundaries, the instantaneous velocity vanishes (nodes); at the midpoint, the amplitude is maximum (antinode).

For the nth allowed helical mode, the pitch satisfies:

$$\lambda_n = \frac{2L}{n}, \quad n = 1, 2, 3, \ldots \tag{4.1}$$

and the wave vector is:

$$k_n = \frac{n\pi}{L}. \tag{4.2}$$

The kinetic energy for non-relativistic velocities becomes:

$$E_n = \frac{p_n^2}{2m} = \frac{n^2 h^2}{8mL^2}, \tag{4.3}$$

which matches the result from the time-independent Schrödinger equation.

4.2. Standing Helices and Quantized Stationary States

Quantized stationary states arise from the superposition of two counter-propagating helices:

$$\mathbf{r}_1 = a_0 e^{ikz}\boldsymbol{\epsilon}_x, \quad \mathbf{r}_2 = a_0 e^{-ikz}\boldsymbol{\epsilon}_x. \tag{4.4}$$

Their superposition gives:

$$\mathbf{r}_{1-2} = a_0(e^{ikz} - e^{-ikz})\boldsymbol{\epsilon}_x = 2ia_0 \sin(kz)\boldsymbol{\epsilon}_x = 2a_0 \sin(kz)\boldsymbol{\epsilon}_y. \tag{4.5}$$

This yields a standing transverse wave with wavefunction:

$$\psi_n(z) = 2a_0 \sin\left(\frac{n\pi z}{L}\right). \tag{4.6}$$

Boundary conditions are naturally satisfied, reproducing the nodal/antinodal structure of quantum mechanics.

Figure 3. The constrained particle can occupy only discrete, quantized closed geodesic paths between two infinite walls separated by a distance L (the infinite potential well). These "standing-wave helices", illustrated in Figure (i), (ii), ... (vi), correspond to the particle traversing the imaginary cylinder once, twice, three times, and so on, respectively, effectively representing frozen patterns of motion in time.

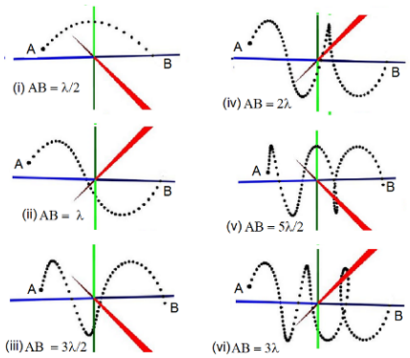

Figure 2

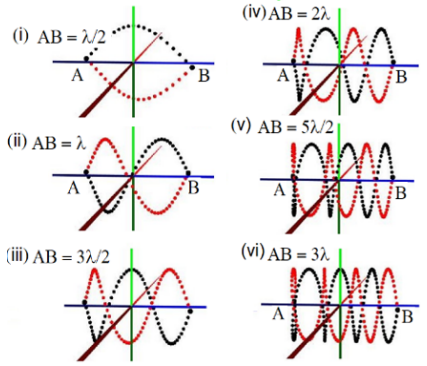

Figure 3

4.3. Phase Coherence and Quantization Condition

A central requirement is that the phase accumulated along a closed trajectory be single-valued:

$$\oint \mathbf{p} \cdot d\mathbf{r} = nh, \quad n \in \mathbb{Z}. \tag{4.7}$$

This generalizes the Bohr-Sommerfeld quantization rule and arises geometrically from closed helical motion [23].

The physical significance of global phase structure in quantum mechanics was firmly established by Berry, who showed that a quantum system acquires a measurable geometric phase when its parameters undergo adiabatic cyclic evolution [24]. The quantization condition in the present helical model may be viewed as a manifestation of the same principle: single-valuedness of the quantum state imposes a topological constraint on the accumulated phase along closed helical geodesics. Quantization thus arises from phase holonomy rather than from imposed boundary conditions.

4.4. Relation to Existing Models

The proposed helical geometry shares conceptual roots with the zitterbewegung interpretations of Hestenes, Barut–Zanghi, Rivas, and Consa. [25–27,29] However, we clarify a distinct shift in emphasis: instead of a classical trajectory, we model the helix as a phase-coherent geodesic. Within this structure, quantization is not a post-hoc assumption

but a necessity of global phase closure, and as we will observe below, the standard operator formalism emerges naturally as the geometric generator of phase evolution. This approach strengthens the work's contextual grounding while explicitly defining its role as a bridge between underlying geometry and observable quantum statistics.

4.5. Superposition and Measurement

The family of standing helices $\{\psi_n\}$ forms a complete orthogonal basis, so any confined state can be expanded as

$$\Psi(z,t) = \sum_n c_n \psi_n(z) e^{-iE_n t/\hbar}. \tag{4.8}$$

In the helical interpretation, these eigenfunctions are not simultaneous superposed states but the set of possible closed helices. A measurement reveals the actual helix occupied by the particle, corresponding to one eigenvalue E_n. Probabilities arise only from ignorance of the initial helical phase, not from intrinsic indeterminacy or wavefunction collapse. This statistical description reflects practical ignorance of initial phase relations and does not constitute a local hidden-variable model, nor does it alter the nonlocal correlations or Bell-inequality violations predicted and observed in standard quantum mechanics.

4.6. Historical and Physical Continuity

This principle of closed helical phase coherence percolates throughout physics: it appears implicitly in Planck's quantized oscillators, explicitly in Bohr's non-radiative orbits, and governs modern quantized phenomena in solids such as phonons, Landau levels, and semiconductor bands. Thus, quantization across quantum and solid-state physics emerges from the same geometric requirement of closed helical standing waves.

5. Principle of Least Action and Helical Geodesics

In classical mechanics, the path of a particle extremizes the action, and in relativity, geodesics extremize proper time. In the helical model, the phase accumulated along the trajectory plays the role of action.

$$S_{\text{helix}} = \int (p \cdot dr - Edt). \tag{5.1}$$

Stationary action corresponds to stationary phase:

$$\delta S_{\text{helix}} = 0. \tag{5.2}$$

This condition ensures that only closed, phase-consistent helices contribute constructively, while all other paths interfere destructively. It is precisely this principle that links the geometric constraint of the helix to the quantization rules of QM.

From this perspective, Feynman's path integral is reinterpreted: instead of summing abstract amplitudes, QM sums over helical trajectories, with only stationary-phase helices surviving as physical states.

6. Spin & Fine Structure from Helical Phase

6.1. Spinor Structure in the Helical Electron Model

In the helical model, the spin-$\frac{1}{2}$ nature arises from the coupling between internal and external motions. The internal rotational frequency is twice the translational frequency, so as the electron advances by one de Broglie wavelength, its internal phase completes two full turns. The wavefunction changes sign after a 2π rotation and returns to its original value only after 4π.

Let the wavefunction be represented as:

$$\Psi(\phi, z) = Ae^{i(kz+\phi/2)}. \tag{6.1}$$

A rotation by 2π yields:

$$\Psi(\phi + 2\pi) = e^{i\pi}\Psi(\phi) = -\Psi(\phi), \tag{6.2}$$

and a 4π rotation restores the phase:

$$\Psi(\phi + 4\pi) = e^{i2\pi}\Psi(\phi) = \Psi(\phi). \tag{6.3}$$

This double-valued behavior mirrors the property of quantum spinors.

6.2. Fine Structure Constant from Helical Geometry

The fine structure constant α arises as a geometric ratio linking internal and external motions:

$$\alpha = \frac{2a_0}{\lambda} = \frac{v}{c}. \tag{6.4}$$

At the Bohr ground state, $v/c \approx 1/137$, giving:

$$\alpha = \frac{e^2}{\hbar c} \approx \frac{1}{137}. \tag{6.5}$$

6.3. Consistency with Pauli Exclusion Principle

The helical model's double-valued phase structure ($\Psi \rightarrow -\Psi$ under 2π rotation) is consistent with the antisymmetry requirement of fermionic wavefunctions. For two electrons in identical helical configurations, phase considerations suggest:

$$\Psi(\mathbf{r}_1, \mathbf{r}_2) \propto -\Psi(\mathbf{r}_2, \mathbf{r}_1), \tag{6.6}$$

which aligns with the Pauli exclusion principle's requirement that the total wavefunction be antisymmetric under particle exchange. This geometric picture complements the standard spin-statistics theorem without replacing its full mathematical formulation.

7. Uncertainty & Quantum Operators

7.1. Geometric Origin of Uncertainty

Here, the electron becomes a 3D object, and the measurements of its instantaneous position and momentum, assuming it to move along a 1D worldline, lead us to the QM uncertainties! The transverse position uncertainty is of order the helical radius:

$$a_0 = \Delta x \approx \pm \frac{\hbar}{2m_0 c}, \tag{7.1}$$

and the conjugate transverse momentum uncertainty is:

$$\Delta p_x \approx \pm m_0 c. \tag{7.2}$$

Thus:

$$\Delta x \Delta p_x \approx \frac{\hbar}{2}, \tag{7.3}$$

consistent with the Heisenberg uncertainty principle.

For heavier particles, $a_0 \to \hbar/(2m_0 c)$ becomes vanishingly small, so the uncertainty shrinks, recovering classical deterministic trajectories. The classical limit emerges naturally within the helical framework. As the particle mass increases, the characteristic transverse scale of the helical motion, of order $\hbar/2mc$, becomes negligibly small compared to macroscopic length scales. In this limit, phase variations average out, the helical structure becomes unresolvable, and the trajectory effectively reduces to that of a point particle following a classical worldline. Thus, classical mechanics is recovered without invoking additional assumptions.

8. Emergent Quantum Operators from Helical Kinematics

In the Helical Electron Model (HEM), the fundamental physical quantity is the phase field $\phi(\mathbf{r}, t)$ associated with the internal helical circulation of the electron. Following de Broglie and Hamilton–Jacobi theory, the phase is related to the classical action S by

$$\phi = \frac{S}{\hbar}. \tag{8.1}$$

In Hamilton–Jacobi theory one has

$$\mathbf{p} = \nabla S, \qquad \frac{\partial S}{\partial t} = -H, \tag{8.2}$$

so that the spatial and temporal derivatives of the phase satisfy

$$\nabla\phi = \frac{\mathbf{p}}{\hbar}, \qquad \frac{\partial\phi}{\partial t} = -\frac{H}{\hbar}, \tag{8.3}$$

where $\mathbf{p}$ is the canonical momentum and H the Hamiltonian.

8.1. Phase Closure and Momentum Quantization

Single-valuedness of the wavefunction around any closed spatial loop C requires the phase-closure condition

$$\oint_C \nabla\phi \cdot d\mathbf{r} = 2\pi n, \qquad n \in \mathbb{Z}. \tag{8.4}$$

Using $\nabla\phi = \mathbf{p}/\hbar$, this immediately yields the Bohr-Sommerfeld quantization condition

$$\oint_C \mathbf{p} \cdot d\mathbf{r} = nh, \tag{8.5}$$

expressing quantization as a geometric constraint on closed helical trajectories.

Consider a phase amplitude of the form

$$\psi(\mathbf{r}, t) = A(\mathbf{r}, t)e^{i\phi(\mathbf{r},t)}. \tag{8.6}$$

Acting with the gradient operator gives

$$\nabla\psi = i(\nabla\phi)\psi + (\nabla A). \tag{8.7}$$

In the semiclassical regime, where the amplitude varies slowly compared to the phase, the second term may be neglected, yielding

$$-i\hbar\nabla\psi \approx \mathbf{p}\psi. \tag{8.8}$$

The momentum operator therefore emerges as

$$\hat{\mathbf{p}} = -i\hbar\nabla, \tag{8.9}$$

acting as the generator of spatial phase translations of the helical mode.

8.2. Gauge Coupling and Intrinsic Phase Circulation

Gauge invariance requires that physical observables depend only on phase differences. Under a gauge transformation, the phase transforms as

$$\phi \to \phi + \frac{e}{\hbar c}\chi, \tag{8.10}$$

which leads directly to the minimal coupling prescription

$$\hat{\mathbf{p}} = -i\hbar\nabla + \frac{e}{c}\mathbf{A}. \tag{8.11}$$

Intrinsic helical circulation associated with spin contributes an additional geometric phase, analogous to a Berry phase, and manifests as spin-dependent corrections to effective momentum and angular momentum operators. No additional dynamical degrees of freedom are introduced.

8.3. Temporal Phase Evolution and the Energy Operator

Temporal evolution of the phase is governed by

$$\frac{\partial\phi}{\partial t} = -\frac{H}{\hbar}. \tag{8.12}$$

For a stationary helical mode with angular frequency ω, the phase evolves as

$$\phi(t) = -\omega t + \phi_0, \tag{8.13}$$

yielding the Planck relation

$$E = \hbar\omega. \tag{8.14}$$

Taking a time derivative of the phase amplitude gives

$$\frac{\partial\psi}{\partial t} = i\frac{\partial\phi}{\partial t}\psi + \frac{\partial A}{\partial t}. \tag{8.15}$$

Neglecting slow amplitude variations leads to

$$i\hbar\frac{\partial\psi}{\partial t} = E\psi, \tag{8.16}$$

from which the energy operator emerges as

$$\hat{E} = i\hbar\frac{\partial}{\partial t}. \tag{8.17}$$

Within the helical interpretation, rest energy corresponds to the intrinsic phase rotation frequency associated with internal luminal circulation.

8.4. Interpretive Summary

In the HEM framework, the canonical quantum operators for momentum and energy are not introduced as independent postulates. Instead, they arise as geometric generators of spatial and temporal phase evolution of phase-coherent helical trajectories. Quantum mechanics is thus recovered as a statistical description of underlying phase geometry, fully consistent with the standard formalism while providing a transparent physical interpretation.

8.5. Ladder Operators as Node Reconfiguration

In systems admitting standing helical modes, the quantized states may be labeled by an integer winding number n corresponding to the number of phase nodes along a closed trajectory. Transitions between adjacent states therefore correspond to the addition or removal of a half-wavelength segment between nodes, $n \to n \pm 1$.

Within the standard operator formalism, such transitions are generated by the ladder operators $\hat{a}^\dagger$ and $\hat{a}$ acting on stationary eigenstates. In the helical interpretation, these operators acquire a geometric meaning: $\hat{a}^\dagger$ increases the winding number by inserting an additional phase node, while $\hat{a}$ removes one. The algebraic properties of ladder operators thus reflect the discrete topology of allowed phase-closed helical configurations rather than independent dynamical assumptions.

This interpretation preserves the standard harmonic-oscillator and atomic transition formalisms while providing a geometric visualization of excitation and de-excitation processes.

8.6. Derivation of Schrödinger and Klein-Gordon Equations

(A) In the non-relativistic regime energy E takes the usual form

$$E = \frac{p^2}{2m} + V(\mathbf{r}), \tag{8.18}$$

where m is the particle's inertial mass and $V(\mathbf{r})$ any external potential. Replace E and $\mathbf{p}$ with their operator equivalents and apply to $\Psi(\mathbf{r}, t)$:

$$i\hbar \frac{\partial}{\partial t}\Psi(\mathbf{r}, t) = \left(\frac{\hat{\mathbf{p}}^2}{2m} + V(\mathbf{r}) \right) \Psi(\mathbf{r}, t). \tag{8.19}$$

Using $\hat{\mathbf{p}}^2 = (-i\hbar\nabla)^2 = -\hbar^2\nabla^2$ we obtain the familiar time-dependent Schrödinger equation:

$$\boxed{i\hbar \frac{\partial \Psi}{\partial t} = -\frac{\hbar^2}{2m}\nabla^2\Psi + V(\mathbf{r})\Psi.} \tag{8.20}$$

(B) Starting from the relativistic energy-momentum relation,

$$E^2 = p^2c^2 + m^2c^4, \tag{8.21}$$

we again replace $E \mapsto i\hbar\partial_t$ and $\mathbf{p} \mapsto -i\hbar\nabla$. Acting on a scalar field $\Psi(\mathbf{r}, t)$ yields

$$\left(i\hbar\frac{\partial}{\partial t}\right)^2 \Psi = \left[(-i\hbar\nabla)^2c^2 + m^2c^4\right]\Psi. \tag{8.22}$$

Rearranging,

$$-\hbar^2\frac{\partial^2\Psi}{\partial t^2} = -\hbar^2c^2\nabla^2\Psi + m^2c^4\Psi,$$

or equivalently the covariant Klein-Gordon equation,

$$\left(\frac{1}{c^2}\frac{\partial^2}{\partial t^2} - \nabla^2 + \frac{m^2c^2}{\hbar^2}\right)\Psi(\mathbf{r}, t) = 0. \tag{8.23}$$

8.6.1. Helical phase interpretation

The derived Klein–Gordon equation,

$$\left(\frac{1}{c^2}\frac{\partial^2}{\partial t^2} - \nabla^2 + \frac{m^2c^2}{\hbar^2}\right)\Psi(\mathbf{r}, t) = 0, \tag{8.24}$$

admits a natural interpretation within the helical framework. The operator $\frac{1}{c^2}\frac{\partial^2}{\partial t^2} - \nabla^2$ acts on the phase field $\phi(\mathbf{r}, t)$ of the internal helical circulation, while the constant term $\frac{m^2c^2}{\hbar^2}$ represents the fixed curvature (torsion) of the helix.

Specifically:

- The wave operator $\frac{1}{c^2}\frac{\partial^2}{\partial t^2} - \nabla^2$ ensures phase coherence across spacetime, encoding the lightlike constraint $ds^2 = 0$ discussed in Section 9.1.
- The mass term $\frac{m^2c^2}{\hbar^2} = \left(\frac{mc}{\hbar}\right)^2$ corresponds to the intrinsic rotation frequency $\omega_0 = 2mc^2/\hbar$ of the internal luminal motion (Section 3.1).
- Solutions $\Psi = Ae^{i\phi}$ represent helical modes whose four-gradient $\partial_\mu\phi = (\frac{1}{c}\frac{\partial\phi}{\partial t}, \nabla\phi)$ satisfies $(\partial_\mu\phi)(\partial^\mu\phi) = \left(\frac{mc}{\hbar}\right)^2$, the relativistic dispersion relation in phase form.

8.7. Time Reversal and Parity

The internal helical motion defines proper time in the particle's rest frame. A wavefunction

$$\psi = Ae^{i\omega t} \tag{8.25}$$

represents counterclockwise (CCW) rotation, i.e. forward in time, while

$$\psi = Ae^{-i\omega t} = Ae^{i\omega(-t)} \tag{8.26}$$

Figure 4. Helical phase evolution with time. To move from position z_0 at time t_0 to z_1 at a later time $t_1 > t_0$ (forward time evolution), the phase advances in the counterclockwise (CCW) direction, corresponding to $e^{+i\omega t}$. To move backward in time to z_2 at $t_2 < t_0$, the phase retraces in the clockwise (CW) direction, corresponding to $e^{-i\omega t}$. The right-handed and left-handed helices thus represent time-reversed trajectories.

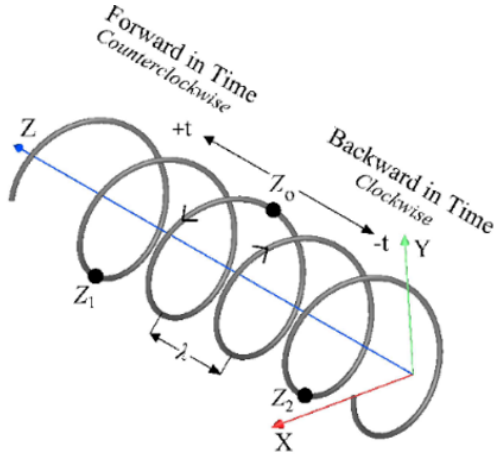

represents clockwise (CW) rotation, i.e. backward in time.

For a free electron moving along the z-axis, the helix traced at z_0 (time t_0) connects to earlier and later positions z_1 and z_2 by CCW and CW rotations, respectively. The two helices are mirror images, corresponding to a parity transformation. Hence, the intrinsic helical structure naturally links time reversal ($t \to -t$) and parity (P) operations, suggesting a geometric visualization of how T and P transformations act on the internal phase structure, without implying fundamental symmetry violation beyond standard theory. [28].

8.8. Relation to Recent Classical Models of Spinning Particles

In a recent preprint, Rivas has addressed the question of whether an electron can be described by the evolution of a single point [29]. By analyzing the geometry of smooth curves in three-dimensional space, he demonstrates that the electron's center of charge may be represented as a point moving continuously at the speed of light and governed by higher-order differential equations. The center of mass emerges as a distinct dynamical point, and the relative motion of the center of charge around the center of mass gives rise to spin and magnetic moment as purely kinematical effects.

These conclusions closely parallel the foundational assumptions of the Helical Electron Model (HEM), in which the electron is described as an internal luminal motion constrained to a helical trajectory. In both approaches, spin is not an abstract quantum degree of

freedom but arises from real internal circulation, and zitterbewegung corresponds to a physical internal motion rather than a mathematical artifact.

The present work, however, extends beyond classical kinematical models by showing how quantum phenomena emerge from geometric phase closure. While Rivas establishes the necessity of internal luminal motion for a consistent description of spin, the HEM demonstrates how quantization, standing-wave states, and the Schrödinger and relativistic wave equations arise from global phase coherence along closed helical geodesics. In this sense, the two approaches are complementary: the former clarifies the classical geometric structure of spinning particles, while the latter provides the missing bridge to quantum mechanics.

9. Geometric Unification of Special Relativity

9.1. Invariance of the Speed of Light and Worldline Geometry

In the helical model, the electron's total motion combines internal circulation and external translation such that the resultant velocity is always luminal. The internal motion occurs in the transverse plane $(x_{\rm int}, y_{\rm int})$ with instantaneous velocity components $\dot{x}_{\rm int}$, $\dot{y}_{\rm int}$, while the external motion along the z-axis has speed v. The combined constraint is

$$\left(\frac{dx_{\rm int}}{dt}\right)^2 + \left(\frac{dy_{\rm int}}{dt}\right)^2 = c^2 - v^2. \tag{9.1}$$

The infinitesimal spacetime interval along the helical path is then

$$ds^2 = dx^2 + dy^2 + dz^2 - c^2dt^2 \tag{9.2}$$

Substituting $dx = dx_{\rm int}$, $dy = dy_{\rm int}$, and $dz = v\,dt$ gives

$$ds^2 = (c^2 - v^2)dt^2 + v^2dt^2 - c^2dt^2 = 0, \tag{9.3}$$

showing that the helical trajectory itself is null (lightlike): the point on the helix moves at the speed of light.

However, the worldline of the electron's center of mass remains timelike, with proper time element $d\tau = dt\sqrt{1 - v^2/c^2}$. The helical trajectory is therefore light-like, while the worldline of the electron's center of mass remains time-like. This dual character—a timelike guiding center traced by a luminal helical motion—provides a natural geometric origin for Lorentz invariance and the constancy of the speed of light.

Figure 5. Relativistic invariance from helical worldline geometry. In the rest frame, the electron exhibits internal circular motion at speed c; in a moving frame, the same motion appears as a helix with reduced internal speed $u = \sqrt{c^2 - v^2}$, keeping the resultant speed invariant at c. This dual light-like and time-like description provides a direct geometric basis for Lorentz invariance and time dilation.

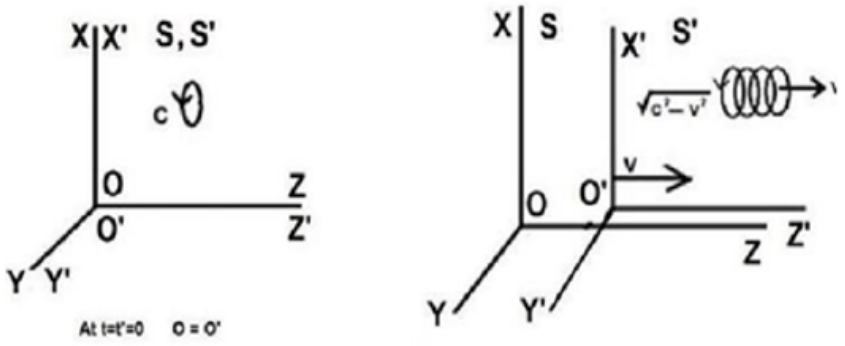

9.2. Time Dilation from Internal Rotation

In the rest frame, the period of internal rotation is

$$T_0 = \frac{2\pi a_0}{c}. \tag{9.4}$$

In a frame where the electron moves with velocity v, the internal tangential speed reduces to $u = \sqrt{c^2 - v^2}$, giving

$$T = \frac{2\pi a_0}{u} = \gamma T_0, \tag{9.5}$$

where $\gamma = 1/\sqrt{1 - v^2/c^2}$. Thus, time dilation follows directly from the reduced internal speed required to preserve the total luminal velocity.

9.3. Length Contraction from Helical Geometry

The axial distance traversed during one complete internal cycle in the moving frame is:

$$\Delta z' = v \cdot T' = v \cdot \gamma T_0 = \gamma v T_0 \tag{9.6}$$

In the rest frame, the axial displacement per cycle is zero (pure rotation). The proper length associated with one cycle — if we imagine marking the endpoints of one cycle in the rest frame and Lorentz transforming — contracts according to the usual length contraction formula. More formally, consider two events corresponding to the same phase point separated by one cycle. Their spacetime interval satisfies $ds^2 = 0$ (lightlike), and the spatial projection in the moving frame contracts exactly as predicted by Lorentz transformations.

9.4. Relativistic Mass and Momentum from Spin Conservation

In the rest frame, the intrinsic spin angular momentum is

$$S = m_0 c a_0, \tag{9.7}$$

where $a_0 = \hbar/2m_0c$. In a moving frame, conservation of spin requires $mua_0 = m_0ca_0$, yielding

$$m = \gamma m_0, \tag{9.8}$$

so the relativistic mass increase emerges dynamically from maintaining constant angular momentum under the constraint of total luminal motion.

9.5. Relativistic Energy and the Meaning of Mass-Energy Equation

The total energy of the electron can be obtained by integrating the work done by a force during acceleration. The incremental work is

$$dE = F\,dz = v\,dp, \tag{9.9}$$

where $p = \gamma m_0 v$ is the relativistic momentum and $\gamma = 1/\sqrt{1 - v^2/c^2}$. Using the relation $dp = m_0\,d(\gamma v)$ and simplifying,

$$dE = v\,dp = v\,m_0\,d(\gamma v) = m_0c^2\,d\gamma. \tag{9.10}$$

Integrating from rest ($\gamma = 1$) to a velocity v gives

$$E = \gamma m_0 c^2. \tag{9.11}$$

The increase in total energy above the rest value represents the kinetic energy,

$$K = E - E_0 = (\gamma - 1)m_0c^2. \tag{9.12}$$

In this interpretation, the rest energy $E_0 = m_0c^2$ represents the kinetic energy of the electron's internal luminal circulation, while the additional term $(\gamma - 1)m_0c^2$ arises from the coupling between this internal rotation and the external translational motion. Hence, the celebrated relation $E = mc^2$ attains a concrete dynamical meaning: it expresses the total kinetic energy of a continuous light-speed motion constituting the electron, rather than merely a conversion factor between mass and energy.

This provides a complementary geometric interpretation of the constancy of c, embedding it within the internal phase structure of electrons, without modifying the postulates or predictions of special relativity.

10. Interference & Measurement

10.1. Double-Slit Interference as a Moiré-like Effect

In the helical-motion framework, interference patterns arise as deterministic Moiré-like effects generated by phase-modulated trajectories [30]. Each slit imprints a geometric phase map on the electron. Let $\Phi_1(x, y)$ and $\Phi_2(x, y)$ denote the phase profiles associated with Slit 1 and Slit 2, determined solely by slit geometry and the electron's momentum.

When an electron passes through Slit 1, it acquires the phase $e^{i\Phi_1(x,y)}$, but the detection process compares this phase with the reference phase $e^{i\Phi_2(x,y)}$ contributed by the alternative path. The resulting probability distribution is

$$P_1(x, y) \propto \left| e^{i\Phi_1(x,y)} + e^{i\Phi_2(x,y)} \right|^2 = 2 + 2\cos[\Phi_1(x, y) - \Phi_2(x, y)]. \tag{10.1}$$

Similarly, if the electron passes through Slit 2, the roles of the phase maps interchange:

$$P_2(x, y) \propto \left| e^{i\Phi_2(x,y)} + e^{i\Phi_1(x,y)} \right|^2 = 2 + 2\cos[\Phi_2(x, y) - \Phi_1(x, y)]. \tag{10.2}$$

Since $\cos(-\theta) = \cos(\theta)$, both contributions produce the same spatial distribution. Thus the total detection profile is

$$P_{\text{tot}}(x, y) \propto 1 + \cos[\Delta\Phi(x, y)], \tag{10.3}$$

where $\Delta\Phi(x, y) = \Phi_1(x, y) - \Phi_2(x, y)$ is the geometrically determined phase difference.

For far-field observation, the usual expression follows from the geometric path difference $d \sin\theta$:

$$I(\theta) \propto 2 + 2\cos(\Delta\phi), \qquad \Delta\phi = \frac{2\pi}{\lambda} d \sin\theta. \tag{10.4}$$

This geometric picture offers an alternative visualization consistent with standard quantum statistics, without altering the role of measurement postulates. or a particle simultaneously traversing both slits. Instead, the interference pattern emerges statistically from many independent electrons, each carrying a definite helical phase and acquiring a deterministic phase map from its slit [31].

The process is directly analogous to the generation of Moiré patterns. Two transparency sheets, each with its own periodic structure (phase maps Φ_1 and Φ_2), may be created at different times and without interacting. When one is placed over the other, a beat pattern (the Moiré envelope) appears purely from the geometric superposition of phases. Likewise, in the double-slit experiment, each electron contributes one phase map, while the apparatus supplies the complementary reference pattern. The interference fringes arise from the deterministic phase geometry, not from any communication or interaction between electrons.

A further consequence of the geometric phase picture is that the interference pattern is sensitive not only to slit separation, but also to the rotation of the slit pair about the beam axis. Such a rotation introduces a transverse phase shear in the maps $\Phi_1(x, y)$ and $\Phi_2(x, y)$, effectively modifying the local phase gradient across each slit. In the helical-trajectory description this corresponds to a controlled twist in the reference phase pattern, leading to a predictable lateral shift or skewing of the interference fringes. This slit-rotation sensitivity follows directly from the Moiré-type phase geometry and is not usually emphasized in the conventional quantum-mechanical treatment, where phase is attributed to a global wavefunction rather than to trajectory-bound phase maps. This description does not imply that single electrons generate classical trajectories observable in individual events, but provides a geometric interpretation consistent with standard quantum statistics.

11. Interpretive Extensions and Conceptual Applications

The helical phase framework developed in this work is intended primarily as a geometric interpretation of established quantum phenomena. In this section, we briefly indicate how the same phase-based picture may offer intuitive insight into several collective and nonlocal effects, without modifying their standard theoretical descriptions.

11.1. Quantum Tunneling as Phase Continuity

In standard quantum mechanics, tunneling arises from the non-vanishing of the wavefunction in classically forbidden regions. Within the helical phase framework, this phenomenon may be interpreted geometrically in terms of phase continuity.

When an electron encounters a potential barrier, the local wave vector becomes imaginary, leading to an exponential decay of the amplitude. However, the phase remains well-defined and continuous across the barrier. In the helical picture, this corresponds to a deformation of the helical trajectory in which classical propagation is suppressed while phase coherence is maintained.

Transmission through the barrier thus reflects the ability of the helical phase to remain matched across regions of reduced amplitude, in full agreement with the standard tunneling probability predicted by quantum mechanics.

11.2. Quantum Jumps as Discrete Phase Reconfiguration

Atomic bound states correspond to standing helical configurations satisfying a global phase-closure condition. Transitions between these states occur when interaction with an external electromagnetic field disrupts the existing phase structure.

In the helical framework, a quantum jump corresponds to a discrete reconfiguration of the standing helical mode into a new phase-closed configuration. Intermediate

configurations that do not satisfy phase closure cannot persist as stationary states and therefore do not appear in observations. The apparent abruptness of quantum jumps thus reflects the discrete topology of allowed phase configurations rather than a breakdown of continuous dynamics.

Energy conservation is ensured through photon absorption or emission, consistent with time-dependent perturbation theory and the standard selection rules.

11.3. Superconductivity and Phase Coherence

In conventional theory, superconductivity arises from the formation of paired electronic states whose collective quantum phase remains coherent over macroscopic distances. In the helical phase framework, such paired states may be visualized as electrons with correlated internal phase circulation, allowing their combined quantum state to maintain long-range phase coherence while propagating through a crystalline lattice.

From this geometric perspective, the suppression of dissipation in superconducting states may be interpreted as a consequence of sustained phase matching between the paired helical modes and the periodic crystal environment. This interpretation is fully consistent with BCS theory and does not introduce additional dynamical assumptions, serving only as a geometric visualization of established coherence phenomena.

11.4. Entanglement as Phase-Locked Correlation

Quantum entanglement is characterized by correlations that cannot be factorized into independent subsystems. Within the helical phase framework, such correlations may be visualized in terms of phase-locked internal structures established during interaction or state preparation.

For two electrons, a correlated phase structure may be written schematically as

$$\psi_i(\mathbf{r}, t) = A_i e^{i(\mathbf{k}_i \cdot \mathbf{r} - \omega_i t + \phi_i)}, \tag{11.1}$$

with the constraint

$$\phi_1 + \phi_2 = \Phi_0 = \text{constant}. \tag{11.2}$$

This relation does not imply hidden variables, predetermined outcomes, or superluminal signaling. This phase-locking description is a visualization of quantum non-separability and should not be interpreted as a hidden-variable mechanism.

11.5. Relation to Prior Internal Motion Models

Internal circulatory models of the electron at the Compton scale have been proposed by several authors, notably Hestenes, Rivas, and Consa. The present work is complementary

to these approaches, emphasizing a helical trajectory interpreted as a constrained geodesic in spacetime. Within this framework, quantization, spin-$\frac{1}{2}$ symmetry, and interference arise from global phase-closure conditions rather than from assumed internal forces.

The formulation further unifies de Broglie periodicity, zitterbewegung, and relativistic kinematics within a single phase-geometric picture, while remaining fully consistent with the standard operator formalism and predictive structure of quantum mechanics.

Thus the helical phase model does not introduce new equations or alter empirical predictions. It provides a *geometric visualization* of the same mathematical structure, aiming to bridge quantum formalism with classical spacetime intuition.

12. Proposed Experimental and Computational Probes

The helical phase framework developed here is fully consistent with established quantum theory and does not require the introduction of new physical interactions or dynamical laws. While no new experimental predictions are claimed, the following probes may offer contexts where the geometric interpretation is especially transparent.Nevertheless, it suggests several avenues in which modern experimental and computational techniques may offer indirect insight into the internal phase structure underlying quantum phenomena, interpreted within this geometric picture.

12.1. Ultrafast Probes and Zitterbewegung-Scale Motion

The intrinsic helical circulation associated with the electron corresponds to the zitterbewegung frequency scale, with a characteristic transverse length of order $\hbar/2mc \sim 10^{-13}\mathrm{m}$. While direct spatial resolution at this scale is currently inaccessible, attosecond streak-camera techniques, ultrafast photoemission, and time-resolved spectroscopy may be sensitive to averaged transverse oscillatory effects through timing offsets, angular distributions, or phase delays [32].

Such measurements would not constitute direct observation of internal motion, but could provide indirect signatures consistent with internal phase dynamics already encoded in relativistic quantum theory.

12.2. Spin-Polarized Compton Scattering

Compton scattering experiments employing spin-polarized electron beams exhibit spin-dependent asymmetries accurately described by relativistic quantum electrodynamics. Within the helical phase framework, these asymmetries admit a geometric interpretation in terms of correlated internal phase circulation and linear momentum.

High-precision measurements of angular, energy, and polarization-dependent scattering cross sections may therefore offer an experimentally accessible context in which the

phase-geometric interpretation can be compared with conventional descriptions.

12.3. Structured Double-Slit Interference

In the helical phase picture, interference phenomena arise from the superposition of phase-coherent helical modes. Modifications of slit geometry—such as varying slit thickness, tilt, or internal structure—introduce controlled phase shear between contributing modes.

These geometrical modifications may generate higher-order modulation or Moiré-like envelope structures superimposed on standard interference fringes. All such effects remain fully consistent with conventional quantum predictions, while providing a useful testing ground for geometric phase interpretations.

12.4. Computational Simulations of Helical Ensembles

Numerical simulations provide a particularly accessible means of exploring the helical phase interpretation. Ensembles of constrained helical trajectories can be simulated to reproduce standard quantum phenomena including interference, tunneling, and decoherence.

Agreement with Schrödinger-based simulations would demonstrate the consistency of the helical framework with established quantum mechanics, while offering additional geometric intuition into phase evolution, coherence, and ensemble behavior.

12.5. Relation to Bell's Theorem and Quantum Nonlocality

The helical phase framework does not introduce hidden variables, additional dynamical degrees of freedom, or superluminal signaling mechanisms. Rather, it emphasizes global phase coherence as an intrinsic feature of quantum states, already present within the standard formalism.

From this perspective, nonlocal quantum correlations may be visualized as arising from shared phase structure established during interaction or state preparation. This geometric viewpoint is analogous to global phase effects observed in the Aharonov-Bohm phenomenon, where physically measurable consequences arise from nonlocal phase relations without violating relativistic causality.

This interpretation remains fully consistent with Bell's theorem and with the experimentally verified violation of Bell inequalities. Measurement outcomes are not attributed to predetermined local values; instead, the helical phase picture provides a visualization of quantum non-separability without altering the statistical predictions or foundational assumptions of quantum mechanics.

13. Conceptual Implications and Future Directions

The helical phase framework developed in this work is intended as a geometric interpretation of established quantum and relativistic formalisms rather than as an alternative theory. In this spirit, several conceptual implications merit brief discussion, particularly with regard to the interpretation of quantum nonlocality, operator structure, and the geometric origin of spinor symmetries.

13.1. Geometric Complement to the Dirac Formalism

The Dirac equation provides an algebraic and relativistically invariant description of spin-$\frac{1}{2}$ particles. The helical phase model offers a complementary geometric visualization in which the mathematical structure of Dirac spinors is associated with internal phase circulation constrained by relativistic kinematics.

Within this interpretation, the algebraic properties of spinors—including the emergence of SU(2) symmetry and the requirement of 4π rotational invariance—are understood as manifestations of an underlying phase geometry rather than of classical spatial rotation. This viewpoint is consistent with the broader recognition that gauge and spinorial structures may arise from geometric phases in internal state space, as emphasized by Wilczek and Zee [33].

The standard Dirac formalism remains unchanged; the helical picture serves solely to clarify its geometric content and to provide physical intuition for otherwise abstract spinorial symmetries.

Mapping between helical phase geometry and Dirac spinors

1. **Four-component spinor as coupled helical modes:** The Dirac spinor $\psi = \begin{pmatrix} \psi_+ \\ \psi_- \end{pmatrix}$ can be interpreted as representing two possible helical chiralities (right-handed and left-handed internal rotations) coupled through the mass term. In the helical model, these correspond to the two possible senses of internal circulation relative to the direction of propagation.

2. **Dirac matrices as rotation generators:** The Dirac matrices γ^μ act as generators of spacetime rotations. In the helical picture:

   - γ^0 (time component) generates internal temporal phase evolution,
   - γ^i (space components) generate spatial rotations of the helical axis,
   - The Clifford algebra $\{\gamma^\mu, \gamma^\nu\} = 2g^{\mu\nu}$ emerges from the geometry of phase-preserving Lorentz transformations.

3. **Zitterbewegung as oscillatory motion between components:** The rapid oscillations in the Dirac equation between positive and negative energy components correspond physically to the electron's internal luminal circulation. The frequency $\omega = 2mc^2/\hbar$ matches the zitterbewegung frequency derived from helical kinematics (Section 3.1).

4. **Spinor transformation under rotation:** Under a spatial rotation by angle θ, Dirac spinors transform as $\psi \to e^{i\boldsymbol{\sigma}\cdot\hat{\mathbf{n}}\theta/2}\psi$, exhibiting the characteristic 4π periodicity. This double-valuedness maps directly to the helical phase requirement that the electron's internal phase completes two full revolutions (4π) for each de Broglie wavelength advance (Section 6.1).

5. **Dirac equation as phase continuity condition:** The free Dirac equation

$$(i\hbar\gamma^\mu\partial_\mu - mc)\psi = 0$$

   can be reinterpreted as a condition for phase coherence along helical worldlines. The mass term mc couples the two chiral helical modes, ensuring consistent phase evolution.

6. **SU(2) symmetry from helical topology:** The SU(2) symmetry of non-relativistic spin emerges naturally from the topology of closed helical paths. The space of phase-coherent helical configurations modulo 4π rotations forms a space homeomorphic to SU(2), providing a geometric basis for spinor representations.

Mathematical correspondence Writing the Dirac spinor in polar form $\psi = \rho e^{iS/\hbar}u$, where ρ is the amplitude, S the classical action, and u a normalized spinor, the helical model identifies:

- $S/\hbar$ as the accumulated helical phase,
- ρ as the envelope of helical amplitude,
- u as encoding the orientation and chirality of internal circulation.

This geometric interpretation remains fully consistent with the standard Dirac formalism while providing physical intuition for otherwise abstract mathematical structures. The helical model thus serves as a "classical picture" of Dirac electron theory, complementing the algebraic formulation with spacetime visualization.

14. Summary and Conclusions

This work has presented a geometric interpretation of electron dynamics based on phase-coherent helical motion constrained by relativistic kinematics. Within this framework, key quantum and relativistic features—such as spin-$\frac{1}{2}$ symmetry, rest energy, quantization, and Lorentz invariance—emerge as interconnected consequences of phase geometry rather than as independent postulates.

The helical phase model does not modify the mathematical structure of quantum mechanics or special relativity. Instead, it provides a complementary physical visualization of their formal elements, clarifying the geometric origin of quantum operators, standing states, interference, tunneling, and quantum transitions. Within this interpretation, the quantum wavefunction functions as a statistical descriptor of ensembles of phase-coherent helical trajectories, fully consistent with standard probabilistic predictions.

Beyond reproducing established results, the framework offers pedagogical value by linking abstract quantum concepts to intuitive geometric structures. It also suggests directions for further investigation, including numerical simulations of constrained helical ensembles and refined experimental probes of phase coherence. Overall, the helical phase interpretation serves as a conceptual bridge between quantum mechanics and relativity, enriching physical intuition while remaining fully aligned with orthodox theory.

Acknowledgements The author acknowledges the use of AI-assisted tools (OpenAI ChatGPT) for language editing and formatting assistance. All conceptual development, analysis, and interpretation are the author's own. The author thanks Prof. Manu Jaiswal and Prof. C. V. Krishnamurthy for valuable discussions, and Mr. M. Saravanan for his assistance in the drawings.

Glossary of Symbols

Table 1. Nomenclature of symbols and physical constants

Symbol	Description	Definition / Value
c	Speed of light in vacuum	2.99×10^8 m/s
h ($\hbar$)	Planck's constant (reduced)	6.626×10^{-34} J·s
m_0	Electron rest mass	9.109×10^{-31} kg
a_0	Transverse helical radius	$\hbar/(2m_0c)$
λ	de Broglie wavelength (Helical pitch)	h/p
ω_0	Zitterbewegung frequency	$2m_0c^2/\hbar$
T_0	Period of internal rotation	$\pi\hbar/(m_0c^2)$
α	Fine-structure constant	$2a_0/\lambda$
γ	Lorentz factor	$(1 - v^2/c^2)^{-1/2}$
ψ	Complex wavefunction	$Ae^{i(kz-\omega t)}$

References

1. L. de Broglie, *Waves and quanta*, Nature **118**, 441–442 (1926).
2. P. A. M. Dirac, *The quantum theory of the electron*, Proc. R. Soc. Lond. A **117**, 610–624 (1928).
3. E. Schrödinger, *Über die kräftefreie Bewegung in der relativistischen Quantenmechanik*, Sitzungsber. Preuss. Akad. Wiss., Phys.-Math. Kl. **24**, 418–428 (1930).
4. A. Einstein, *On the electrodynamics of moving bodies*, in *The Principle of Relativity* (Methuen and Company, London, 1923), pp. 35–65.
5. Natarajan, T. S. *A Unified Conceptual Foundation for Relativity and Quantum Mechanics*. Physics Essays, **9**(2), 301–310.
6. T. S. Natarajan, *Does the 'complex' wave function in QM represent anything 'real' at all?*, Quantum Speculations **5**(3), 1–15 (2023).
7. A. P. French, *Special Relativity* (W. W. Norton, New York, 1968).
8. E. F. Taylor and J. A. Wheeler, *Spacetime Physics*, 2nd ed. (W. H. Freeman, San Francisco, 1992).
9. J. N. Bahcall and S. Bahcall, *The Sun's motion perpendicular to the galactic plane*, Nature **316**, 706–708 (1985).
10. O. Consa, *The helical model—our solar system is a vortex* (2014), https://oliverconsa.com.
11. D. R. Gies and J. W. Helsel, *Ice age epochs and the Sun's path through the galaxy*, Nature **317**, 338–341 (2005).
12. R. B. Stothers, *Terrestrial record of the Solar System's oscillation about the galactic*

plane, Nature **317**, 338–341 (1985).
13. H. C. Berg and R. A. Anderson, *Bacteria swim by rotating their flagellar filaments*, Nature **245**, 380–382 (1973).
14. B. M. Friedrich, I. H. Riedel-Kruse, J. Howard, and F. Jülicher, *High-precision tracking of sperm swimming fine structure provides strong test of resistive force theory*, J. Exp. Biol. **213**, 1226–1234 (2010).
15. J. J. L. Higdon, *The hydrodynamics of flagellar propulsion: Helical waves*, J. Fluid Mech. **94**, 331–351 (1979).
16. H. Wada and R. R. Netz, *Hydrodynamics of helical-shaped bacterial motility*, Phys. Rev. E **80**, 021921 (2009).
17. E. Lauga and T. R. Powers, *The hydrodynamics of swimming microorganisms*, Rep. Prog. Phys. **72**, 096601 (2009).
18. D. Hestenes, *The zitterbewegung interpretation of quantum mechanics*, Found. Phys. **20**, 1213–1232 (1990).
19. M. Rivas, *Classical relativistic spinning particles*, J. Math. Phys. **30**, 318–328 (1989).
20. O. Consa, *The helical electron model*, Prog. Phys. **14**, 80–89 (2018).
21. A. Gray, *Modern Differential Geometry of Curves and Surfaces with Mathematica*, 2nd ed. (CRC Press, Boca Raton, 1998).
22. J. J. Sakurai and J. Napolitano, *Modern Quantum Mechanics*, 2nd ed. (Pearson, San Francisco, 2011).
23. N. Bohr, *On the constitution of atoms and molecules*, Philos. Mag. **26**, 1–25 (1913).
24. M. V. Berry, "Quantal phase factors accompanying adiabatic changes," *Proceedings of the Royal Society of London A* **392**, 45–57 (1984).
25. D. Hestenes, Zitterbewegung in quantum mechanics, *Found. Phys.* **38**, 788-816 (2008).
26. A. O. Barut and N. Zanghi, Classical model of the Dirac electron, *Phys. Rev. Lett.* **52**, 2009-2012 (1984).
27. M. Rivas, *Kinematical Theory of Spinning Particles*, Kluwer Academic (2001).
28. C. S. Wu, E. Ambler, R. W. Hayward, D. D. Hoppes, and R. P. Hudson, *Experimental test of parity conservation in beta decay*, Phys. Rev. **105**, 1413–1415 (1957).
29. M. Rivas, "Is it possible to describe an electron by the evolution of a single point?" *arXiv:2601.11597* [physics.gen-ph] (2026), https://doi.org/10.48550/arXiv.2601.11597.
30. P. G. Merli, G. F. Missiroli, and G. Pozzi, *On the statistical aspect of electron interference phenomena*, Am. J. Phys. **44**, 306–307 (1976).
31. A. Tonomura, J. Endo, T. Matsuda, T. Kawasaki, and H. Ezawa, *Demonstration of single-electron buildup of an interference pattern*, Am. J. Phys. **57**, 117–120 (1989).
32. F. Krausz and M. Ivanov, *Attosecond physics*, Rev. Mod. Phys. **81**, 163–234 (2009).
33. F. Wilczek and A. Zee, "Appearance of gauge structure in simple dynamical systems,"

Physical Review Letters **52**, 2111–2114 (1984).